



Deliverable Report

Deliverable No: D1.2

Deliverable Title: INTERMEDIATE QPM SPDC

Grant Agreement number: **255914**

Project acronym: **PHORBITECH**

Project title: **A Toolbox for Photon Orbital Angular Momentum Technology**

Project website address: **www.phorbitech.eu**

Name, title and organization of the scientific representative of deliverable's lead beneficiary (task leader):

Dr Juan P. Torres
ICFO - Institut De Ciencies Fotoniques
Castelldefels, Spain

Deliverable table

Deliverable no.	D1.2
Deliverable name	Intermediate QPM SPDC
WP no.	1
Lead beneficiary no.	3 (ICFO)
Nature	R
Dissemination level	PU
Delivery date from Annex I	Month 12
Actual delivery date	30 September 2011

D1.2 Intermediate QPM SPDC: Intermediate report with a first analysis of the performances of the transverse quasi-phase-matching (QPM) approach for OAM SPDC generation. Quasi-phase-matching will be achieved by modulating the material composition and structure, as well as by tailoring the pump beam transverse profile, and spectral and/or temporal shape.
[Excerpt from GA-Annex I DoW]

1. THE ROLE OF TRANSVERSE QUASI-PHASE MATCHING

The main advantage of using a nonlinear crystal with transverse QPM is to generate new types of quantum states with orbital angular momentum, even though the flux of down-converted photons generated might be reduced. For the sake of simplicity, let assume a short crystal where the diffraction of the pump beam, and the signal and idler photons, can be neglected. In this case, the quantum state of the down-converted photons can be written as

$$|\Psi\rangle = \int d\vec{r}_1 d\vec{r}_2 F(\vec{q}_1, \vec{q}_2) a_1^+(\vec{q}_1) a_2^+(\vec{q}_2)$$

$$F(\vec{q}_1, \vec{q}_2) = \int dx dy \chi(\vec{r}_\perp) E_p(\vec{r}_\perp) \exp[-i(\vec{q}_1 + \vec{q}_2) \cdot \vec{r}_\perp]$$

where χ is the transverse varying nonlinear coefficient of the crystal, and E_p is the pump beam profile. We notice that now, the nature of the quantum state is determined by the multiplication of the pump beam and the nonlinear coefficient (χE_p). If the nonlinear coefficient is constant, we recover the usual result

$$|\Psi\rangle = \int d\vec{q}_1 d\vec{q}_2 \hat{E}_p(\vec{q}_1 + \vec{q}_2) a_1^+(\vec{q}_1) a_2^+(\vec{q}_2)$$

In usual configurations, if the pump beam is Gaussian, the probability to project the down-converted photons into Gaussian modes is higher than projecting into higher order modes (see the paper mentioned in the following section). The question is: Can we make use of transverse QPM to modify this? Can we devise a spatial transverse pattern χ so that the maximum efficiency takes place for a higher order mode? Some simple calculations show that the efficiency of generation of modes with indexes l_1 and p_1 , and l_2 and p_2 is given by:

$$P_{l_2, p_2}^{l_1, p_1} = \left| \int d\vec{r}_\perp \chi(\vec{r}_\perp) E_p(\vec{r}_\perp) U_{l_1, p_1}^*(\vec{r}_\perp) U_{l_2, p_2}(\vec{r}_\perp) \right|^2$$

The effect of the transverse QPM configuration is to generate an effective pump beam which modifies the characteristics of the down-converted photons.

Let us consider the simple transverse QPM structure depicted in Figure 1.

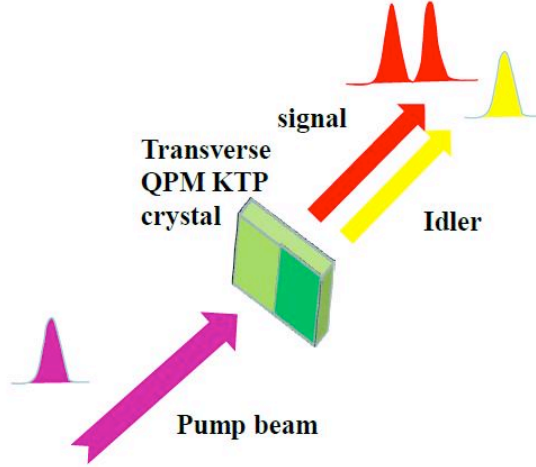


Figure 1. Transverse QPM configuration, where the nonlinear coefficient is positive for half the nonlinear crystal ($x>0$), and negative for the other half ($x<0$).

In this case, since the nonlinear function is now an odd function, the expansion of the down converted photons in terms of OAM modes does not contain paired photons in Gaussian Modes. It remains to be explored which are the optimum configurations for specific applications.

2. ROLE OF THE PUMP BEAM SHAPE IN THE EFFICIENCY OF SPDC

Let us consider the excitation of a second-order nonlinear crystal with an intense pump beam, so that pairs of photons entangled in the spatial degree of freedom (orbital angular momentum, OAM) are generated by means of spontaneous parametric down conversion (SPDC). The main requirement of the source is that it should offer a high output flux. More specifically:

- We aim at generating entanglement in a 2×2 dimensional space (such it is the Hilbert space spanned by the polarization degree of freedom alone). This is the case of quantum states that make use of the polarization and OAM degrees of freedom and are of the form

$$|\Psi\rangle = \frac{1}{\sqrt{2}} \left(|R; m = +1\rangle_1 |L; m = -1\rangle_2 + |L; m = -1\rangle_1 |R; m = +1\rangle_2 \right) \quad (1)$$

Here sub-index 1 and 2 refer to two distinguishable photons (for instance, photons with different frequency or different direction of propagation). The symbols R,L stands for right-handed (left-handed) circular polarization and $m=+1,-1$ represent Laguerre-Gauss modes with winding numbers $m=-1,+1$ and radial index $p=0$.

- We aim for high efficiency. Typical experiments in quantum optics count photon coincidences after the photons have traversed appropriately designed optical systems, which reveal the properties of interest of the quantum state generated. SPDC is a

highly inefficient process, so that even under optimum conditions, quantum optics experiments barely show efficiencies greater than 10^{-7} . Therefore, once determined the spatial modes of interest in a particular application, it is of great interest to optimize the SPDC process so that most of the photons generated belong to the ensemble of modes of interest.

In order to generate quantum states with the sought-after correlations, and implement high efficiency sources of entangled photons, the SPDC configurations considered in this report will make use of:

- **A Collinear configuration:** the pump beam, and the photons generated (signal and idler) propagate along the same direction in the nonlinear crystal. Increasing the efficiency usually require focusing the pump beam into a narrow spot. Non-collinear configurations are not so easily handled under tight focusing of all waves involved.
- **A Non-critical configuration:** We assume a direction of propagation inside the nonlinear crystal so that all waves do not show Poynting-vector walk-off, i.e. *spatial walk-off*. Under tight focusing conditions, the presence of spatial walk-off (*critical configuration*) produces undesirable spatial correlations between the paired photons.
- **Quasi-phase matching:** Taking into account the two conditions stated above, in most cases, it is necessary to use the technique called quasi-phase matching (QPM) to fulfill the necessary phase-matching condition between the pump, signal and idler waves. In QPM, the sign of the nonlinear coefficient of the crystal alternate periodically between positive and negative values. Moreover, the use of QPM usually allows the use of the highest nonlinear coefficient of the nonlinear medium, which results in the corresponding increase of the efficiency.

3. ENHANCING THE EFFICIENCY OF OAM ENTANGLEMENT

In the SPDC configuration considered here, and given a specific nonlinear crystal with a length L , the design parameters are:

- The beam waist of the pump beam (indicated as w_p).
- The beam waist of the collection mode (indicated as w_s).

The question is:

Once chosen a specific target (*spatial modes*), what is the optimum configuration (values of w_p and w_s) that maximizes the flux of down-converted photons generated?

The answer is reported in the paper (which is part of the present deliverable):

Silvana Palacios, R. de J. Leon-Montiel, Martin Hendrych, Alejandra Valencia and Juan P. Torres, *Flux enhancement of photons entangled in orbital angular momentum*, Optics Express **19**, 14108 (2011).

For generating a quantum state of the form given in Eq. (1), the optimum configuration is given in the Figure. In this case, an estimated 82% of all photons generated (see Eq. 26 of the paper) belong to the Hilbert space of interest. For instance, let us consider a degenerate SPDC process in a $L = 20$ mm PPKTP nonlinear crystal with nonlinear coefficient $\chi^{(2)}=10$ pm/V, pumped by

a CW pump at $\lambda_p = 405$ nm and refractive indices $n_p = n_1 = n_2 = 1.8$. If the total losses of the optical systems are $\eta = 0.1$, the spectral brightness F is

$$F = \gamma P_p (mW) \text{ with } \gamma \sim 1 \times 10^5 \text{ photons/s/nm/mW}$$

Here P_p is the pump power. Comparing with the flux of down-converted photons measured in other experiments that also make use of the quantum state given by Eq. (1), we see that by properly choosing the optimum value of the pump beam waist w_p and the optimum size of the collection mode w_s , one could observe a noteworthy enhancement of the spectral brightness of the source.

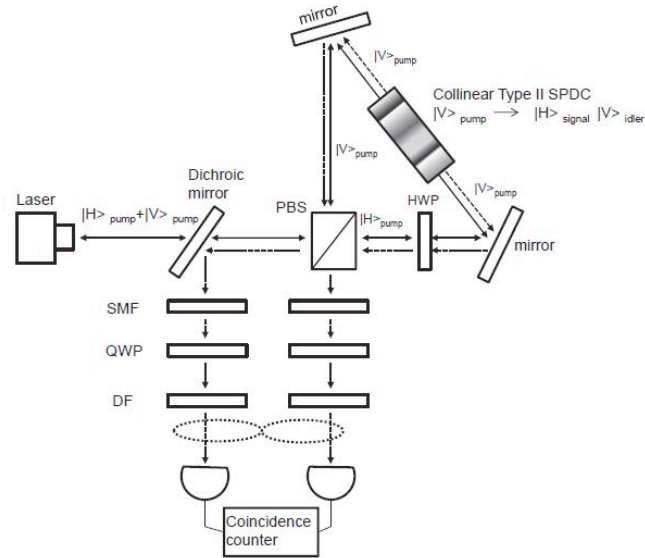


Figure 1: Scheme of the combination of a type-II SPDC source embedded in a Sagnac interferometer and diffractive elements to generate photons entangled in the polarization and spatial degrees of freedom with maximum efficiency. SMF: Single-mode fiber; QWP: Quarter-wave plate; HWP: Half-wave plate; PBS: Polarization beam splitter; DF: Diffractive element. The linked dot lines represent the existence of entanglement.

Flux enhancement of photons entangled in orbital angular momentum

Silvana Palacios,¹ R. de J. León-Montiel,¹ Martin Hendrych,¹
Alejandra Valencia,¹ and Juan P. Torres^{1,2,*}

¹ICFO-Institut de Ciències Fotoniques, Mediterranean Technology Park, 08860 Castelldefels (Barcelona), Spain

²Dept. Signal Theory and Communications, Universitat Politècnica de Catalunya, Jordi Girona 1-3, 08034 Barcelona Spain

*juanp.torres@icfo.es

Abstract: Entangled photons are generally collected by detection systems that select their certain spatial modes, for example using single-mode optical fibers. We derive *simple* and *easy-to-use* expressions that allow us to maximize the coupling efficiency of entangled photons with specific orbital angular momentum (OAM) correlations generated by means of spontaneous parametric downconversion. Two different configurations are considered: one in which the beams with OAM are generated by conversion from beams without OAM, and the second when beams with OAM are generated directly from the nonlinear medium. Also, an example of how to generate a maximally entangled qutrit is presented.

© 2011 Optical Society of America

OCIS codes: (190.4410) Nonlinear optics, parametric processes; (270.0270) Quantum optics.

References and links

1. J. T. Barreiro, N. K. Langford, N. A. Peters, and P. G. Kwiat, "Generation of hyperentangled photon pairs," *Phys. Rev. Lett.* **95**, 260501 (2005).
2. E. Nagali, L. Sansoni, L. Marrucci, E. Santamato, and F. Sciarrino, "Experimental generation and characterization of single-photon hybrid ququarts based on polarization and orbital angular momentum encoding," *Phys. Rev. A* **81**, 052317 (2010).
3. G. Molina-Terriza, J. P. Torres, and L. Torner, "Twisted photons," *Nat. Phys.* **3**, 305–310 (2007).
4. A. Mair, A. Vaziri, G. Weihs, and A. Zeilinger, "Entanglement of the orbital angular momentum states of photons," *Nature* **412**, 313–316 (2001).
5. B. Dayan, A. Pe'er, A. A. Friesem, and Y. Silberberg, "Nonlinear interactions with an ultrahigh flux of broadband entangled photons," *Phys. Rev. Lett.* **94**, 043602 (2005).
6. C. Kurtsiefer, M. Oberparleiter, and H. Weinfurter, "High-efficiency entangled photon pair collection in type-II parametric fluorescence," *Phys. Rev. A* **64**, 023802 (2001).
7. F. A. Bovino, P. Varisco, A. M. Colla, G. Castagnoli, G. Di Giuseppe, and A. V. Sergienko, "Effective fiber-coupling of entangled photons for quantum communication," *Opt. Commun.* **227**, 343–348 (2003).
8. M. Pelton, P. Marsden, D. Ljunggren, M. Tengner, A. Karlsson, A. Fragemann, C. Canalias, and F. Laurell, "Bright, single-spatial-mode source of frequency non-degenerate, polarization-entangled photon pairs using periodically poled KTP," *Opt. Express* **12**, 3573–3580 (2004).
9. D. Ljunggren, and M. Tengner, "Optimal focusing for maximal collection of entangled narrow-band photon pairs into single-mode fibers," *Phys. Rev. A* **72**, 062301 (2005).
10. R. S. Bennink, "Optimal collinear Gaussian beams for spontaneous parametric down-conversion," *Phys. Rev. A* **81**, 053805 (2010).
11. A. Fedrizzi, T. Herbst, A. Poppe, T. Jennewein, and A. Zeilinger, "A wavelength-tunable fiber-coupled source of narrowband entangled photons," *Opt. Express* **15**, 15377–15386 (2007).
12. J. P. Torres, A. Alexandrescu, and L. Torner, "Quantum spiral bandwidth of entangled two-photon states," *Phys. Rev. A* **68**, 050301 (2003).

13. H. Di Lorenzo Pires, H. C. B. Florijn, and M. P. van Exter, "Measurement of the spiral spectrum of entangled two-photon states," *Phys. Rev. Lett.* **104**, 020505 (2010).
14. E. Nagali, F. Sciarrino, F. De Martini, L. Marrucci, B. Piccirillo, E. Karimi, and E. Santamato, "Quantum information transfer from spin to orbital angular momentum of photons," *Phys. Rev. Lett.* **103**, 013601 (2009).
15. J. P. Torres, Y. Deyanova, L. Torner, and G. Molina-Terriza, "Preparation of engineered two-photon entangled states for multidimensional quantum information," *Phys. Rev. A* **67**, 052313 (2003).
16. C. I. Osorio, G. Molina-Terriza, and J. P. Torres, "Correlations in orbital angular momentum of spatially entangled paired photons generated in parametric down-conversion," *Phys. Rev. A* **77**, 015810 (2008).
17. R. Loudon, *The Quantum Theory of Light* (Oxford University Press, 1973).
18. A. Gatti, R. Zambrini, M. San Miguel, and L. A. Lugiato, "Multiphoton multimode polarization entanglement in parametric down-conversion," *Phys. Rev. A* **68**, 053807 (2003).
19. W. Wasilewski, A. I. Lvovsky, K. Banaszek, and C. Radzewicz, "Pulse squeezed light: simultaneous squeezing of multiple modes," *Phys. Rev. A* **73**, 063819 (2006).
20. S. P. Walborn, A. N. de Oliveira, S. Padua, and C. H. Monken, "Multimode Hong-Ou-Mandel interference," *Phys. Rev. Lett.* **90**, 143601 (2003).
21. L. Marrucci, C. Manzo, and D. Paparo, "Optical spin-to-orbital angular momentum conversion in inhomogeneous anisotropic media," *Phys. Rev. Lett.* **96**, 163905 (2006).
22. T. Kim, M. Fiorentino, and F. N. C. Wong, "Phase-stable source of polarization-entangled photons using a polarization Sagnac interferometer," *Phys. Rev. A* **73**, 012316 (2006).
23. W. P. Grice, R. S. Bennink, D. S. Goodman, and A. T. Ryan, "Spatial entanglement and optimal single-mode coupling," *Phys. Rev. A* **83**, 023810 (2011).
24. P. J. Winzer and W. R. Leeb, "Fiber coupling efficiency for random light and its applications to lidar," *Opt. Lett.* **23**, 986–988 (1998).
25. F. Fidler and O. Wallner, "Application of single-mode fiber-coupled receivers in optical satellite to high-altitude platform communications," *EURASIP J. Wireless Commun. Netw.* **2008**, 864031 (2008).

1. Introduction

Spontaneous parametric downconversion (SPDC), a nonlinear optical process in which two lower-frequency photons (signal and idler) are generated when a strong pump interacts with the atoms of a nonlinear material, is a reliable source for generating pairs of entangled photons. When SPDC is properly engineered, the photon pairs can be entangled in any degree of freedom: polarization, frequency, space or time. The entanglement can reside in one degree of freedom, or can also be shared between them [1,2]. In the case of the spatial degree of freedom, spatial entanglement can be depicted as residing in the quantum correlations between spatial modes that bear orbital angular momentum (OAM) [3]. The use of the OAM of photons allows the generation of quantum states in a high-dimensional Hilbert space [4].

In general, one of the drawbacks of SPDC is that the flux of generated paired photons is very low. For instance, Dayan et al. [5] generated an ultra-high flux of downconverted photons ($\sim 0.3\mu\text{W}$), that even while being orders of magnitude greater than what is typically utilized in quantum optics experiments, it still shows an efficiency of only $\sim 10^{-7}$. In order to increase the flux of paired photons, one has to choose longer nonlinear materials or materials with higher nonlinear coefficients.

Moreover, any experimental detection system selects only part of the total number of generated photon pairs. Therefore, to increase the flux of paired photons, one should also add to the optimization toolkit the use of the most appropriate configuration that collects as many photons as possible without disturbing the sought-after quantum correlations between them. For instance, in most SPDC sources that generate photons entangled in polarization, the signal and idler photons are collected with single-mode optical fibers before being detected. In this case, the goal is then to maximize the coupling efficiency of paired photons into the fundamental Gaussian mode of the fiber. A number of studies have established some basic rules to optimize the efficiency of these particular SPDC configurations [6–10] and several experiments have confirmed some of the predictions [11]. However, a similar study to optimize the collection efficiency of entangled photons with OAM has not been reported.

In this paper, we address the question of what is the optimum SPDC configuration, i.e., the

pump beam waist and the size of the collection mode for a given crystal length, that maximizes the flux of entangled photons that exhibit specific OAM correlations. For this, it is necessary to calculate the spiral spectrum of the photons generated in SPDC, i.e., the decomposition of the biphoton mode function in a basis of spatial modes with OAM. Even though the decomposition has been calculated [12] and experimentally demonstrated [13], the implications of the engineering of the spiral spectrum for enhancing the flux of paired photons in selected SPDC configurations have not yet been fully explored.

Along these lines, we will consider two scenarios. On the one hand, the case where OAM correlations are generated by making use of *spin-orbital* coupling devices that starting from polarization entangled photons with a Gaussian spatial shape, generate photon pairs with OAM and polarization correlations [14]. In this case, to increase the flux it is necessary to maximize the generation of pairs of photons with a Gaussian spatial shape. On the other hand, we can make use of the OAM correlations that are directly harvested at the output face of the nonlinear crystal [15]. This is necessarily the case if the goal is to generate quantum states in multidimensional Hilbert spaces. Here the aim is to maximize the generation of photons with specific non-Gaussian spatial shapes.

The paper is organized as follows. In Section 2, we derive the main equations that lay the foundations of our analysis. In Section 3, we obtain the optimum configuration that maximizes the generation and coupling efficiency of photon pairs into single-mode optical fibers. In Section 4, we address the enhancement of the flux when downconverted photons are projected into Laguerre-Gaussian spatial modes.

2. General equations

Let us consider a periodically-poled nonlinear crystal of length L and nonlinear coefficient $\chi^{(2)}$ illuminated by a continuous wave (CW) pump beam, with central frequency ω_p . All the interacting waves (the pump, signal and idler) propagate along the same direction (*collinear configuration*), and the signal-idler pairs can be distinguished because either they show orthogonal polarizations or because they have different central frequencies. We consider a non-critical configuration, i.e., neither of the interacting waves experiences a Poynting-vector walk-off. The absence of spatial walk-off allows one to employ longer nonlinear media. Narrowband filters are located in front of the single-photon counting modules that detect in coincidence the arrival of a pair of photons.

The spatial distribution of the pump beam at the center of the nonlinear crystal, in the transverse wavevector domain, writes

$$E_p(\mathbf{q}) = E_0 (q_x + iq_y)^{m_p} \exp(-|\mathbf{q}|^2 w_p^2 / 4), \quad (1)$$

which corresponds to a beam with an OAM of $m_p \hbar$ per photon. $\mathbf{q} = (q_x, q_y)$ is the transverse wavevector and w_p is the beam waist. E_0 is a normalizing constant, so that $\int d\mathbf{q} |E_p(\mathbf{q})|^2 = 1$.

The signal and idler photons are projected into specific spatial modes before detection. The use of Laguerre-Gaussian modes ($U_{m,p}$) allows one to describe the spatial quantum correlations of the paired photons in a straightforward and clear way. The Laguerre-Gaussian modes are characterized by two integer indices, p and m . The positive index p is the radial index, and the winding number m , which can be any integer number, determines the azimuthal phase dependence of the mode, which is of the form $\sim \exp(im\varphi)$. The functions $U_{m,p}$ are normalized, i.e., $\int d\mathbf{q} |U_{m,p}(\mathbf{q})|^2 = 1$.

The use of a collinear configuration and the absence of spatial walk-off makes hold the selection rule $m_p = m_1 + m_2$. Here m_p is the optical vortex winding number of the pump beam, and m_1 and m_2 are the winding numbers of the modes into which the quantum states of the signal and idler photons are projected, respectively. The configuration considered here allows

to establish clear spatial correlations between the photons in terms of modes with OAM. For instance, if the pump beam has a Gaussian spatial shape ($m_p = 0$), only paired photons with $m_1 = -m_2$ can be detected in coincidence. It is important to remark that this might not be the case for other non-collinear or critical SPDC configurations [16].

Most analyses of the spatial characteristics of photons entangled in OAM usually follow the Schrödinger picture, where it is the quantum state that evolves in time. The quantum theoretical analysis presented in this paper will use the Heisenberg picture, where it is the signal and idler field operators, a_1 and a_2 , that evolve as a function of the propagation distance inside the nonlinear medium. In the Heisenberg picture, *all* the coherence functions of interest can be easily calculated, even when a first-order approximation of the quantum evolution equations is used, as it is the case here [17].

In the framework of the Heisenberg picture, the propagation equations for the signal and idler operators are given by [18]

$$\begin{aligned}\frac{\partial a_1(\mathbf{q}_1, z)}{\partial z} &= -i\tilde{\sigma} \int d\mathbf{q}_2 a_2^\dagger(\mathbf{q}_2, z) E_p(\mathbf{q}_1 + \mathbf{q}_2) \\ &\quad \times \exp[ik_p(\mathbf{q}_1 + \mathbf{q}_2) - ik_1(\mathbf{q}_1) - ik_2(\mathbf{q}_2)], \\ \frac{\partial a_2(\mathbf{q}_2, z)}{\partial z} &= -i\tilde{\sigma} \int d\mathbf{q}_1 a_1^\dagger(\mathbf{q}_1, z) E_p(\mathbf{q}_1 + \mathbf{q}_2) \\ &\quad \times \exp[ik_p(\mathbf{q}_1 + \mathbf{q}_2) - ik_1(\mathbf{q}_1) - ik_2(\mathbf{q}_2)],\end{aligned}\quad (2)$$

where the dimensionless nonlinear coefficient $\tilde{\sigma} = \sigma \sqrt{F_p}$ writes

$$\tilde{\sigma} = \left[\frac{\hbar \omega_1 \omega_2 \omega_p [\chi^{(2)}]^2 F_p}{32\pi^2 \epsilon_0 c^3 n_1(\omega_1) n_2(\omega_2) n_p(\omega_p)} \right]^{1/2}. \quad (3)$$

\mathbf{q}_1 and \mathbf{q}_2 are the transverse wavenumbers of the signal and idler photons, respectively, and $\omega_1 = \omega_2 = \omega_p/2$ are the central frequencies. n_i ($i = p, 1, 2$) are the refractive index at the corresponding central frequency, $k_i(\mathbf{q}) = (\omega_i^2 n_i^2/c^2 - |\mathbf{q}|^2)^{1/2}$ are the longitudinal wavevectors and F_p is the total flux (photons/s) of pump photons that traverse the nonlinear crystal.

The quantities $\langle a_1^\dagger(\mathbf{q}_0) a_1(\mathbf{q}_0) \rangle \Delta \mathbf{q}$ and $\langle a_2^\dagger(\mathbf{q}_0) a_2(\mathbf{q}_0) \rangle \Delta \mathbf{q}$ designate the spectral brightness (photons/s/Hz) of signal and idler photons, respectively, generated with transverse wavenumbers between $\mathbf{q}_0 - \Delta \mathbf{q}/2$ and $\mathbf{q}_0 + \Delta \mathbf{q}/2$. Therefore, the overall spectral brightness is

$$F = \int d\mathbf{q} \langle a_1^\dagger(\mathbf{q}) a_1(\mathbf{q}) \rangle. \quad (4)$$

We are interested in calculating the spectral brightness F^{m_1, p_1, m_2, p_2} of photons that are detected in coincidence, when the signal photon is projected into a spatial mode with index (m_1, p_1) and the idler photon is projected into a spatial mode with index (m_2, p_2) . The nature and strength of the correlations between paired photons projected into specific spatial modes is determined by the second-order correlation function between signal and idler photons

$$G_{12}^{(2)}(m_1, p_1, m_2, p_2) = \langle b_{m_1, p_1}^\dagger c_{m_2, p_2}^\dagger c_{m_2, p_2} b_{m_1, p_1} \rangle, \quad (5)$$

where b_{m_1, p_1} and c_{m_2, p_2} are operators acting on the signal and idler photons, respectively, that write

$$\begin{aligned}b_{m_1, p_1} &= \int d\mathbf{q} U_{m_1, p_1}(\mathbf{q}) a_1(\mathbf{q}), \\ c_{m_2, p_2} &= \int d\mathbf{q} U_{m_2, p_2}(\mathbf{q}) a_2(\mathbf{q}).\end{aligned}\quad (6)$$

The second-order correlation function given by Eq. (5) can be written in terms of the first-order correlation functions $\langle a_1^\dagger(\mathbf{q})a_1(\mathbf{q}') \rangle$, $\langle a_2^\dagger(\mathbf{q})a_2(\mathbf{q}') \rangle$ and $\langle a_1^\dagger(\mathbf{q})a_2^\dagger(\mathbf{q}') \rangle$ as

$$G_{12}^{(2)}(m_1, p_1, m_2, p_2) = F_1^{m_1, p_1} F_2^{m_2, p_2} + F_{1,2}^{m_1, p_1, m_2, p_2}, \quad (7)$$

where

$$\begin{aligned} F_1^{m_1, p_1} &= \int d\mathbf{q}_1 d\mathbf{q}'_1 U_{m_1, p_1}^*(\mathbf{q}_1) U_{m_1, p_1}(\mathbf{q}'_1) \langle a_1^\dagger(\mathbf{q}_1) a_1(\mathbf{q}'_1) \rangle, \\ F_2^{m_2, p_2} &= \int d\mathbf{q}_2 d\mathbf{q}'_2 U_{m_2, p_2}^*(\mathbf{q}_2) U_{m_2, p_2}(\mathbf{q}'_2) \langle a_2^\dagger(\mathbf{q}_2) a_2(\mathbf{q}'_2) \rangle \end{aligned} \quad (8)$$

are the spectral brightness of signal and idler photons detected after projection into spatial modes with indices (m_1, p_1) and (m_2, p_2) , respectively, and $F_{1,2}^{m_1, p_1, m_2, p_2} = |f_{12}^{m_1, p_1, m_2, p_2}|^2$, where

$$f_{12}^{m_1, p_1, m_2, p_2} = \int d\mathbf{q}_1 d\mathbf{q}_2 U_{m_1, p_1}(\mathbf{q}_1) U_{m_2, p_2}(\mathbf{q}_2) \langle a_1(\mathbf{q}_1) a_2(\mathbf{q}_2) \rangle. \quad (9)$$

In most situations of interest, the nonlinearity is weak. In this case, one can describe the evolution of the signal and idler operators with first-order approximations in the nonlinear coefficient [19], so that the first-order correlation functions can be written as

$$\begin{aligned} \langle a_1^\dagger(\mathbf{q}_1) a_1(\mathbf{q}'_1) \rangle &= \int d\mathbf{q}_2 \Phi^*(\mathbf{q}_1, \mathbf{q}_2) \Phi(\mathbf{q}'_1, \mathbf{q}_2), \\ \langle a_1(\mathbf{q}_1) a_2(\mathbf{q}_2) \rangle &= \Phi(\mathbf{q}_1, \mathbf{q}_2). \end{aligned} \quad (10)$$

The biphoton or mode function writes

$$\Phi(\mathbf{q}_1, \mathbf{q}_2) = \tilde{\sigma} L E_p(\mathbf{q}_1 + \mathbf{q}_2) \text{sinc} \left[\frac{\Delta_k L}{2} \right], \quad (11)$$

where $\Delta_k = k_p(\mathbf{q}_1 + \mathbf{q}_2) - k_1(\mathbf{q}_1) - k_2(\mathbf{q}_2) - K_g$ is the phase-matching function, $K_g = 2\pi/\Lambda$ is the grating vector of the periodically-poled crystal and Λ is the period of the nonlinear grating.

If we make use of the paraxial approximation $k_i(\mathbf{q}) \sim k_i^0 - |\mathbf{q}|^2/(2k_i^0)$ ($i = p, 1, 2$), where k_i^0 is the wavenumber at the corresponding central frequency, and of the condition $n_p \cong n_1 \cong n_2$, we obtain [20]

$$\Delta_k \sim \frac{|\mathbf{q}_1 - \mathbf{q}_2|^2}{2k_p^0}. \quad (12)$$

Finally, using Eqs. (9), (10) and (11), the spectral brightness $F_{12}^{m_1, p_1, m_2, p_2}$ can be written as

$$F_{12}^{m_1, p_1, m_2, p_2} = \left| \int d\mathbf{q}_1 d\mathbf{q}_2 \Phi(\mathbf{q}_1, \mathbf{q}_2) U_{m_1}^*(\mathbf{q}_1) U_{m_2}^*(\mathbf{q}_2) \right|^2. \quad (13)$$

Using Eqs. (4) and (10), the total spectral brightness F can be calculated

$$F = \int d\mathbf{q}_1 d\mathbf{q}_2 |\Phi(\mathbf{q}_1, \mathbf{q}_2)|^2. \quad (14)$$

Additionally, using Eq. (12), we obtain

$$F = \frac{\pi^2 \sigma^2 F_p k_p^0}{2} L. \quad (15)$$

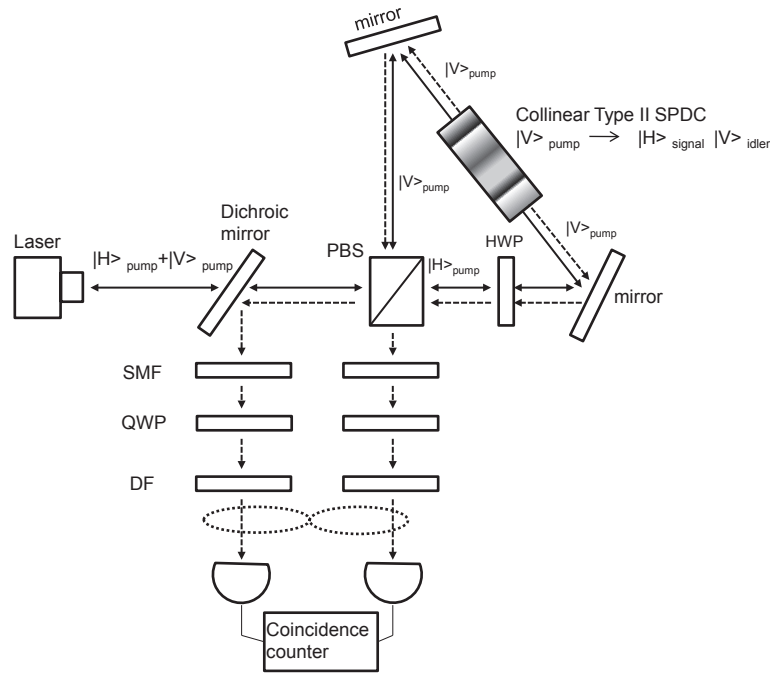


Fig. 1. Scheme of the combination of a type-II SPDC source embedded in a Sagnac interferometer and diffractive elements to generate photons entangled in the polarization and spatial degrees of freedom. SMF: Single-mode fiber; QWP: Quarter-wave plate; HWP: Half-wave plate; PBS: Polarization beam splitter; DF: Diffractive element. The linked dot lines represent the existence of entanglement.

F depends on the total flux of pump photons F_p that traverse the nonlinear crystal, but not on the specific spatial shape of the pump beam. Notice also that it increases linearly with the length of the crystal.

The role of $F_{12}^{m_1, p_1, m_2, p_2}$ as the spectral brightness of interest here is more clearly revealed when we notice that

$$F = \sum_{m_1, p_1, m_2, p_2} F_{12}^{m_1, p_1, m_2, p_2}. \quad (16)$$

To obtain Eq. (16), one has to make use of the completeness relationship $\sum_{m_1, p_1, m_2, p_2} U_{m_1, p_1}(\mathbf{q}_1) U_{m_1, p_1}^*(\mathbf{q}_2) = \delta(\mathbf{q}_1 - \mathbf{q}_2)$.

Regarding the spatial shape of the projection modes $U_{m, p}$, in what follows we will restrict ourselves to the case $p_1 = p_2 = 0$. The spatial shape of the LG modes in which the signal and idler photons will be projected, $U_m \equiv U_{m, p=0}$ writes

$$U_m(\mathbf{p}) = \left(\frac{w_s^2}{2\pi|m|!} \right)^{1/2} \left(\frac{w_s|\mathbf{p}|}{\sqrt{2}} \right)^{|m|} \exp(-|\mathbf{p}|^2 w_s^2 / 4) \exp(im\phi). \quad (17)$$

In order to simplify the notation, we will designate $F_{12}^{m_1, m_2} \equiv F_{12}^{m_1, p_1=0, m_2, p_2=0}$

3. Generation of two-photon entangled states with correlations in polarization and OAM

Let us consider the generation of a quantum state entangled in the polarization and OAM degrees of freedom of the form [14]

$$|\Psi\rangle = \frac{1}{\sqrt{2}} \{ |R, m_1 = 1\rangle_1 |L, m_1 = -1\rangle_2 + |L, m_1 = -1\rangle_1 |R, m_1 = 1\rangle_2 \}, \quad (18)$$

where R and L represent right-handed and left-handed circular polarizations, respectively. The procedure to generate such a state consists of two steps. First, a polarization entangled state embedded in Gaussian modes is generated. And second, properly designed diffractive elements are used to transform the polarization and spatial shape of the photons. For instance, one can use a diffractive element that performs the following transformation [21]:

$$\begin{aligned} |R, m = 0\rangle &\Rightarrow |L, m = +1\rangle, \\ |L, m = 0\rangle &\Rightarrow |R, m = -1\rangle. \end{aligned} \quad (19)$$

The configuration used to generate the quantum state given by Eq. (18) makes use of a non-collinear SPDC configuration with a type-II BBO crystal. The use of a such a non-collinear configuration, which also shows spatial walk-off, prevents from using long crystals to enhance the spectral brightness, since in that case the degree of polarization entanglement would decrease.

A possibility to overcome such a limitation is to use a non-critical collinear SPDC configuration with a Sagnac interferometer ([22], see Fig. 1). In this case, the pump beam induces the generation of pairs of photons with orthogonal polarizations that propagate clock-wise or counter-clockwise in the Sagnac interferometer. Before any polarization or OAM transformation takes place, the quantum state of the generated paired photons can be written as

$$|\Psi\rangle = \frac{1}{\sqrt{2}} \int d\mathbf{q}_s d\mathbf{q}_i \Phi(\mathbf{q}_s, \mathbf{q}_i) \{ |H\rangle_1 |V\rangle_2 + |V\rangle_1 |H\rangle_2 \}. \quad (20)$$

The absence of spatial walk-off allows the use of long crystals, and since the spatiotemporal shape of the generated photons is the same for photons propagating clock-wise or counter-clockwise, no spatiotemporal compensation is necessary after the signal and idler photons leave the interferometer.

Paired photons generated in the quantum state given by Eq. (20) are projected into Gaussian modes. The coupling efficiency of interest in this case is $P_{0,0} = F_{12}^{0,0}/F$. With the help of Eqs. (11), (13) and (15), we obtain

$$P_{00} = \frac{16k_p^0 w_p^2}{\pi L} \left[\frac{w_s^2}{2w_p^2 + w_s^2} \arctan\left(\frac{2L}{k_p w_s^2}\right) \right]^2. \quad (21)$$

In order to maximize the flux of generated paired photons, we should choose optimum values of the pump beam waist (w_p^{opt}) and signal beam waist (w_s^{opt}) that maximize the coupling efficiency $P_{0,0}$. It reaches its maximum value when the conditions

$$w_s^{opt} = \sqrt{2} w_p^{opt} \quad (22)$$

$$\frac{1}{2} \arctan(\alpha) = \frac{\alpha}{1 + \alpha^2} \quad \text{with } \alpha = \frac{L}{k_p^0 (w_p^{opt})^2} \quad (23)$$

are fulfilled. The non-zero value of α that fulfills Eq. (23) is easily found to be $\alpha = 1.39$. This solution gives us the optimum value of the pump beam waist,

$$w_p^{opt} = \sqrt{\frac{L}{\alpha k_p^0}}, \quad (24)$$

Equations (22) and (24) give us the optimum values of the pump beam waist and the collection system that maximizes the number of generated photons with the desired spatial shape.

Some authors [9, 11, 23] make use of the parameters $\xi_p = L/z_p$ and $\xi_s = L/z_s$, where $z_p = k_p^0 w_p^2/2$ and $z_s = k_s^0 w_s^2/2$ are the Rayleigh ranges of the pump and signal waves. With these parameters, the result given by Eq. (24) can be rewritten in terms of ξ_p and ξ_s , so that the optimum values are $\bar{\xi}_p^{opt} = \bar{\xi}_s^{opt} = 2.8$.

Figure 2(a) shows the optimum value of the waist of the collection beam, namely \bar{w}_s , that yields the maximum value of coupling efficiency $P_{0,0}$ for a given value of the pump beam waist w_p . Figure 2(b) shows the maximum value of $P_{0,0}$ for each value of the pump beam waist. We see that for all lengths, the global maximum of $P_{0,0}$ is $P_{0,0}^{max} \sim 82\%$. However, as expected from Eq. (24), the optimum value of the pump beam waist depends on the length of the crystal. In Fig. 2(a) we also plot the condition $w_s = \sqrt{2}w_p$. In both figures, we consider two different values of the nonlinear crystal length: $L = 10$ mm and $L = 20$ mm.

As we have demonstrated above, the *global* maximum of $P_{0,0}$ is obtained for $w_p^{opt} = L/(\alpha k_p^0)$ and $w_s^{opt} = \sqrt{2}w_p^{opt}$. However, if we fix a value of the pump beam different from the optimum value, i.e., $w_p \neq w_p^{opt}$, the optimum size of the signal collection system that maximizes the efficiency (\bar{w}_s), no longer fulfills the condition $\bar{w}_s = \sqrt{2}w_p$. We can observe this in Fig. 2(a). For $w_p = w_p^{opt}$, the condition is fulfilled (open circles), and it corresponds to a global maximum of the coupling efficiency (open circles) in Fig. 2(b). But for larger values of the pump beam ($w_p > w_p^{opt}$), \bar{w}_s is indeed smaller than $\sqrt{2}w_p$, whereas for smaller values ($w_p < w_p^{opt}$), \bar{w}_s is larger than $\sqrt{2}w_p$. In other words, \bar{w}_s yields a local maximum of the coupling efficiency for a fixed value of w_p . To highlight the different coupling efficiency achieved when $w_s = \bar{w}_s$ and when $w_s = \sqrt{2}w_p$, we plot both cases in Fig. 2(b).

The maximum value of collection efficiency $P_{0,0}$ that can be achieved with a pump beam waist given by Eq. (24) and collection system $w_s = \sqrt{2}w_p$, is

$$P_{0,0}^{max} = \frac{4}{\alpha\pi} (\tan^{-1}\alpha)^2, \quad (25)$$

which yields $P_{0,0}^{max} = 82.1\%$. Maximally, some 82% of photons can be collected into a Gaussian mode. This is a universal value that does not depend on the crystal length.

This maximum value is obtained because we are approximating the exact field of the fiber's fundamental mode with a Gaussian function. It is expected that when considering the exact field, the coupling efficiency would decrease. This is analogical to what happens with single-mode fiber-coupled receivers in optical free-space communications [24]: When the optical input field is focused in a single-mode fiber, the maximum coupling efficiency is $\eta_{max} = 81.5\%$ if the field of the fundamental mode of the fiber is approximated by a Gaussian function. On the other hand, if the exact form of the fundamental mode is used [25], the maximum coupling efficiency turns out to be $\eta_{max} = 78.6\%$.

As an example of the usefulness of the results obtained in this section, let us estimate the spectral brightness that can be achieved in the considered SPDC configuration. If η accounts for all the losses of the experimental set-up, i.e., efficiency of the diffractive elements, losses of the singlemode-fibers and quantum efficiency of the detectors, the spectral brightness $\bar{F} = P_{0,0}^{max} \eta F$ of generated paired photons is

$$\bar{F} = 0.41\eta\pi^2\sigma^2 F_p k_p^0 L. \quad (26)$$

For example, let us consider a degenerate SPDC process in a $L = 20$ mm PPKTP nonlinear crystal with nonlinear coefficient $\chi^{(2)} \sim 10$ pm/V, pumped by a CW pump at $\lambda_p = 405$ nm and refractive indices $n_p \simeq n_1 \simeq n_2 = 1.8$. If the total losses of the optical systems are $\eta = 0.1$, the

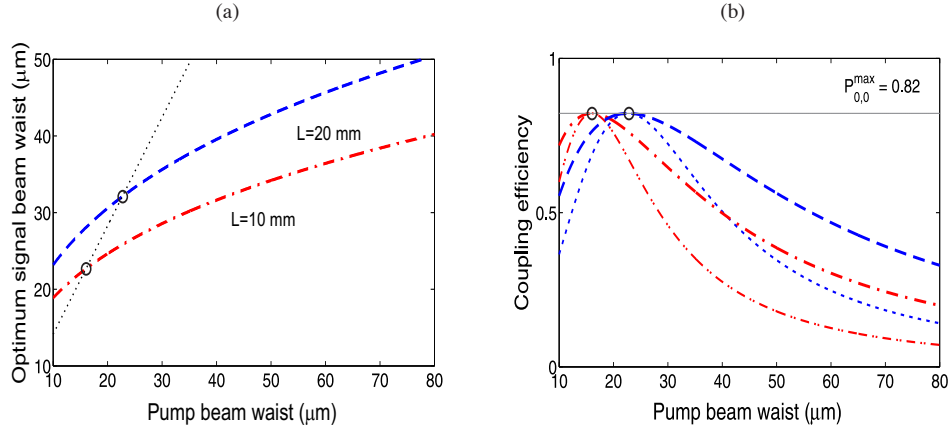


Fig. 2. (a) Optimum beam waist of the collection mode, \bar{w}_s that maximizes the coupling efficiency $P_{0,0}$ for a given pump beam waist w_p for two different nonlinear crystal lengths (blue dashed line: $L = 20$ mm ; red dash-dotted line: $L = 10$ mm). The dotted line represents the condition $w_s = \sqrt{2}w_p$. The open circles designate the values when $w_p = w_p^{opt}$. (b) Maximum coupling efficiency $P_{0,0}$ as a function of pump beam waist w_p . Blue dashed line: maximum for $L = 20$ mm when the optimum value of w_s shown in Fig. 2(a) is used. Red dash-dotted line: maximum for $L = 10$ mm when the optimum value of w_s in Fig. 2(a) is used. Blue (dotted) and red (dash dot-dotted) lines show the coupling efficiency when the signal beam waist is $w_s = \sqrt{2}w_p$ for $L = 20$ mm and $L = 10$ mm, respectively. Horizontal line: Maximum value of $P_{0,0}$ for any crystal length. The open circles designate the global maxima of $P_{0,0}$, when $w_p = w_p^{opt}$.

spectral brightness is $\bar{F} = \gamma P_p (mW)$, where $\gamma \sim 1 \times 10^5$ photons/s/nm/mW and P_p is the pump power. Comparing with the flux of downconverted photons measured in [14], we see that by properly choosing the optimum value of the pump beam waist w_p and the optimum size of the collection mode w_s , one could observe a noteworthy enhancement of the spectral brightness of the source.

4. Generation of two-photon entangled states with OAM correlations

In the previous section, we considered the maximization of the spectral brightness of photons entangled in the polarization degree of freedom with a Gaussian spatial shape. Even though the entanglement in the polarization degree of freedom is transformed to entanglement in the polarization and OAM degrees of freedom, the dimension of the working Hilbert space is still $d = 2$. If the goal is to generate entanglement in a multidimensional Hilbert space ($d > 2$), we can take advantage of the OAM correlations directly generated in the process of SPDC (see Fig. 3).

In this section, first a general calculation is performed to show how to maximize the coupling efficiency of photons with OAM and then an example of how to employ it to generate a maximally entangled qutrit is presented.

Let us consider an SPDC process pumped by a beam with OAM winding number m_p . The two-photon state, which is entangled in the OAM degree of freedom, can be written as

$$|\Psi\rangle = \sum_{m_1} C_{m_1, m_2} |m_1\rangle_1 |m_2\rangle_2, \quad (27)$$

where $F_{12}^{m_1, m_2} = |C_{m_1, m_2}|^2$ is the weight of each mode of the decomposition with $m_p = m_1 + m_2$.

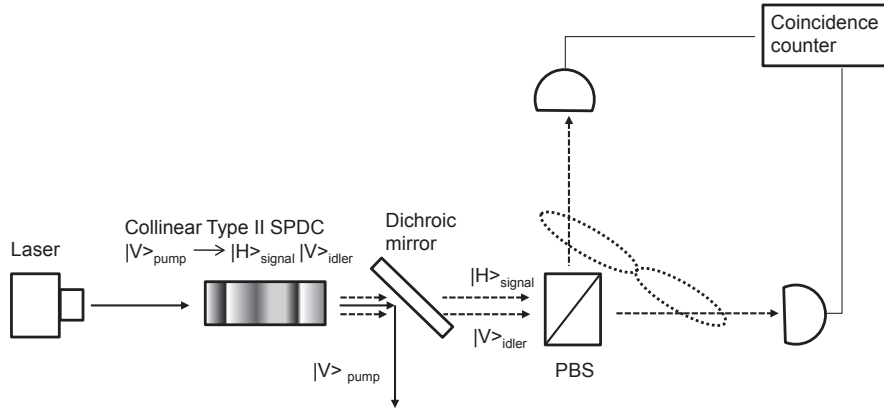


Fig. 3. Scheme of a type-II SPDC configuration for generating photons entangled in the OAM degree of freedom. Photons in Laguerre-Gaussian modes are directly produced in the nonlinear crystal and later separated by a polarization beam splitter (PBS). The linked dot lines represent the existence of entanglement.

In this section, the goal is to maximize the overall coupling efficiency $P = \sum_{m_1, m_2} P_{m_1, m_2}$ for a selected set of values of m_1 , where $P_{m_1, m_2} = F_{12}^{m_1, m_2} / F$.

When projecting the paired photons into non-Gaussian modes, two cases should be considered. Firstly, the case when the winding numbers m_1 and m_2 have the same sign, i.e., $\text{sgn}(m_1) \cdot \text{sgn}(m_2) = 1$, and secondly, the case with $\text{sgn}(m_1) \cdot \text{sgn}(m_2) = -1$. The first situation corresponds, for instance, to cases where the pump beam, and the signal and idler modes are described by Laguerre-Gaussian modes with positive indices m_p , m_1 and m_2 . Making use of Eqs. (13) and (15), we obtain

$$P_{m_1, m_2} = \frac{16k_p^0 w_s^2}{\pi L} \frac{m_p!}{m_1! m_2!} \left[\frac{w_p w_s}{2w_p^2 + w_s^2} \right]^{2m_p+2} \left[\tan^{-1} \left(\frac{2L}{k_p^0 w_s^2} \right) \right]^2. \quad (28)$$

Notice that by setting $m_p = m_1 = m_2 = 0$, we recover Eq. (21).

Inspection of Eq. (28) shows that the optimum signal and idler mode widths are obtained when $w_s = \sqrt{2}w_p$ and $L/(k_p w_p^2) = \alpha$, as in Section 3. The maximum coupling efficiency is now

$$P_{m_1, m_2}^{max} = \frac{m_p!}{8^{m_p} m_1! m_2!} \frac{4}{\alpha \pi} (\tan^{-1} \alpha)^2. \quad (29)$$

Notice that in this case the coupling efficiency of coincidence rates between signal and idler photons into higher-order modes decreases as $P_{m_1, m_2}^{max} / P_{0,0}^{max} = m_p! / (8^{m_p} m_1! m_2!)$, when com-

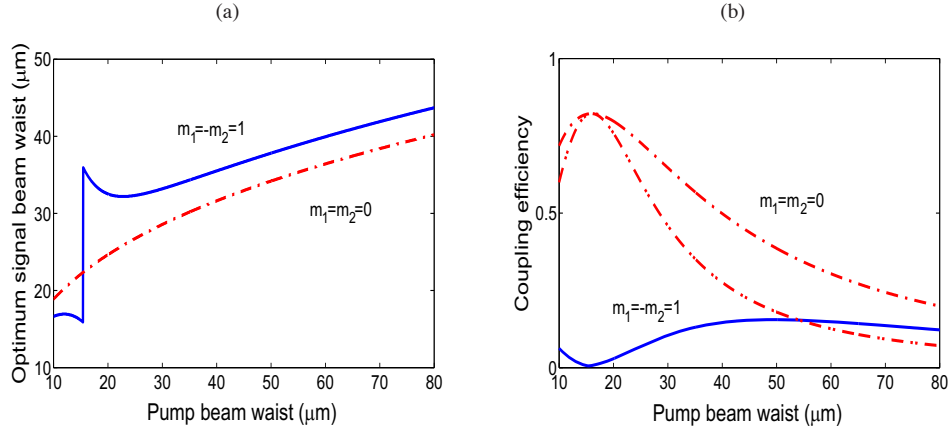


Fig. 4. (a) Optimum beam waist of the collection mode w_s that maximizes the coupling efficiency $P_{1,-1}$ for a given pump beam waist (blue solid line). For the sake of comparison, the optimum beam waist of the collection mode that maximizes the coupling efficiency $P_{0,0}$ for a given pump beam waist is also plotted (red dash-dotted line). (b) Maximum coupling efficiency $P_{1,-1}$ as a function of pump beam waist. Blue solid line: maximum coupling efficiency $P_{1,-1}$ when the optimum value of w_s , as shown in Fig. 4(a), is used. For the sake of comparison, we also plot the coupling efficiency $P_{0,0}$ for two cases. Red dash-dotted line: maximum coupling efficiency $P_{0,0}$. Red dash-dot-dotted line: coupling efficiency when the signal beam waist is $w_s = \sqrt{2}w_p$. The nonlinear crystal length is $L = 10$ mm in all cases.

pared with the case of the projection of the signal and idler photons into Gaussian modes. For instance, for a pump beam with $m_p = 1$, the fraction of signal photons with $m_1 = 0$ detected in coincidence with idler photons with $m_2 = 1$ is $P_{1,0}^{max} = P_{0,1}^{max} \sim 0.1$. For $m_p = 2$, we obtain $P_{2,0}^{max} = P_{0,2}^{max} \sim 0.013$ and $P_{1,1}^{max} \sim 0.026$.

Results are different for the case $\text{sgn}(m_1) \cdot \text{sgn}(m_2) = -1$. For a Gaussian pump beam ($m_p = 0$), the coupling efficiency is given by a somehow more cumbersome expression that writes

$$P_{m,-m} = \frac{4^{1-m} k_p^0 w_p^2}{(m!)^2 \pi L} \left[\frac{2w_s^2}{2w_p^2 + w_s^2} \right]^{2m+2} \left| \sum_{p=0}^m (-1)^p \left[\frac{m!}{p!(m-p)!} \right]^2 \right. \\ \left. \times \frac{\Gamma(m-p+1)\Gamma(p)}{\left[(w_s^2/8)^2 + (L/4k_p^0)^2 \right]^{p/2}} \left[\frac{w_p^2}{4} + \frac{w_s^2}{8} \right]^p \sin \left\{ p \arctan \left(\frac{2L}{k_p^0 w_s^2} \right) \right\} \right|^2. \quad (30)$$

Without loss of generality, let us consider that the signal and idler modes are projected into spatial modes with $m_1 = 1$ and $m_1 = -1$. In this case, Eq. (30) can be written as

$$P_{1,-1} = \frac{16k_p^0 w_p^2 w_s^8}{\pi L (2w_p^2 + w_s^2)^4} \left| \arctan \left(\frac{2L}{k_p^0 w_s^2} \right) - \frac{2k_p^0 L (2w_p^2 + w_s^2)}{4L^2 + (k_p^0 w_s^2)^2} \right|^2. \quad (31)$$

The qualitative behaviour of $P_{1,-1}$ turns out to be quite different from the previously considered cases, where m_1 and m_2 had the same sign. This can be clearly observed in Fig. 4(b), which shows the maximum coupling efficiency that can be achieved as a function of the pump beam waist, when the optimum value of w_s , given by Fig. 4(a), is chosen. Figure 4(b) also shows the optimum value of $P_{0,0}$ (red dash-dotted line), and $P_{0,0}$ when setting $w_s = \sqrt{2}w_p$ (red dash-dot-dotted line).

As an example of the application of the results depicted in Fig. 4(b), let us consider a detection system that projects the generated photons into a particular form of the state given by Eq. (27) in a three-dimensional Hilbert subspace

$$|\Psi\rangle = C_{0,0}|m_1 = 0\rangle_1|m_2 = 0\rangle_2 + C_{-1,1}\{|m_1 = -1\rangle_1|m_2 = 1\rangle_2 + C_{-1,1}|m_1 = 1\rangle_1|m_2 = -1\rangle_2\}, \quad (32)$$

where

$$C_{0,0} = \int d\mathbf{q}_s d\mathbf{q}_i \Phi(\mathbf{q}_s, \mathbf{q}_i) U_0(\mathbf{q}_s) U_0(\mathbf{q}_i), \quad (33)$$

$$C_{-1,1} = \int d\mathbf{q}_s d\mathbf{q}_i \Phi(\mathbf{q}_s, \mathbf{q}_i) U_1(\mathbf{q}_s) U_{-1}(\mathbf{q}_i). \quad (34)$$

The detection arrangement of such a state would be as follows. The generated paired photons show orthogonal polarizations, so they can be separated with a polarizing beam splitter, as shown in Fig. 3. To detect a specific spatial mode with winding number $m_{1,2} = -1, +1$, we can make use of a properly designed hologram of order $M = +1, -1$, or a spatial light modulator. The hologram projects the incoming photons into outgoing photons (in reflection or transmission) that propagate along the first diffraction order of the hologram, and have a winding number $m + M$. After the hologram, a single-mode fiber detects photons with a Gaussian shape, i.e., with winding number $m + M = 0$. For instance, if $M = +1$, detection of a photon after traversing the single-mode fiber implies the presence of an incoming photon with winding number $m = -1$, since any other incoming photon with a different winding number would not be allowed to propagate inside the single-mode fiber.

Notice that the beam waists w_s^0 and w_s^1 of the modes U_0 and U_1 in Eq. (33) can be different to achieve a maximum efficiency. In the detection arrangement described above, the beam waist of the modes detected can be controlled by modifying the optical coupling system of light into the single-mode fiber. The weights of each mode, $P_{0,0} = |C_{0,0}|^2$ and $P_{1,-1} = P_{-1,1} = |C_{-1,1}|^2$ can be read in Fig. 4(b). To generate a maximally entangled qutrit, i.e., a quantum state that fulfills the condition $P_{1,-1} = P_{0,0}$, one has to use specific values of w_p and w_s . For instance, from Fig. 4(b), we can see that if we make use of the condition $w_s = \sqrt{2}w_p$, the value of $w_p \sim 55$ μm where the curves intersect corresponds to a high-flux configuration for a maximally-entangled qutrit with $P_{0,0} = P_{-1,1}$. For this value of w_p , the quantum state given by Eq. (32) represents roughly a 46% of the whole parameter space, i.e., $P_{0,0} = P_{-1,1} = \sqrt{0.46/3}$, which is the coupling efficiency of this particular SPDC configuration. That means that by choosing appropriate values of w_p , w_s^0 and w_s^1 , the coupling efficiency of the projection into a maximally-entangled quantum state of the form given by Eq. (32) can reach a value of 46 %.

5. Conclusions

We have presented an analysis of how to design optimum SPDC configurations that maximize the coupling efficiency of entangled photon pairs with specific OAM correlations in detection systems sensitive to the spatial shape of photons. Collinear non-critical SPDC configurations have been considered, as they facilitate the use of longer nonlinear crystals with the corresponding enhancement of the flux of the generated photons. Furthermore, they allow for a simpler description of the quantum spatial correlations of the two-photon states in terms of spatial modes that bear orbital angular momentum.

The optimization consists in shaping the spiral spectrum of the two-photon state by choosing appropriate values of the pump beam waist (w_p) and the waist of the collection mode (w_s).

If the aim is to generate a quantum state that bears quantum correlations in the OAM and polarization degrees or freedom, the optimum approach is to maximize the flux of polarization

entangled photons projected into Gaussian modes and then transform them into modes with OAM using diffractive elements, such as holograms. We have found that fraction of photon pairs that can be detected under ideal conditions can approach a value of $\sim 82\%$.

On the other hand, if the aim is to generate higher-dimensional quantum states, we have to maximize the spectral brightness of photons with a Laguerre-Gaussian shape directly coming out of the nonlinear material. In the case of a maximally-entangled qutrit, a coupling efficiency of $\sim 46\%$ can be achieved.

Acknowledgments

This work was supported by the Government of Spain (Consolider Ingenio CSD2006-00019, FIS2010-14831). The project PHORBITECH acknowledges the financial support of FET programme, under FET-Open grant number: 255914. This work was also supported in part by FONCICYT project 94142.